Journal of Engineering Research **Vol. 6 No. (2) June 2018 pp.** *209-231*

Adaptive control simulation to optimize metal removal for rough turning

A. M. Alaskari* and S. E. Oraby

Department of Manufacturing Engineering Technology, College of Technological Studies, PAAET, P.O. Box 42325, Shuwaikh 70654, Kuwait

**Corresponding Author: aalaskari@gmail.com*

ABSTRACT

In conventional numerical control machining, it is not possible to change the preset operating parameters in the program during the machining cycle. In contrast, the adaptive control technique uses real-time sensing to continuously and instantaneously adjust the operative feed and/or the speed parameters to their optimal levels in order to ensure a more productive operation. In this study, a model-based adaptive control simulation strategy is proposed to optimize metal removal during rough turning by efficiently utilizing the available power resources within a safe machining environment. The approach is based on recursive continuous iterations to predict the instantaneous level of edge wear, together with the corresponding cutting forces and the consumed power, by considering the relevant models. The best speed-feed pair that provides the maximum metal removal rate without violating the imposed forces and power constraints is selected. Procedures are repeated for subsequent cut intervals by considering cumulative edge wear from preceding intervals until the accumulated edge wear level reaches the specified criterion value. The performance of the proposed model-based method was verified through comparisons with several conventional fixed-parameter wear-time methods. Results proved the superiority of the proposed AC disparate-parameter procedures in terms of noticeable greater productivity as the entire available machine power was exploited with a safe machining environment with reduced cost of the replacement cycle.

Keywords: adaptive control; consumed power; cutting forces; cutting tool wear; metal removal rate.

INTRODUCTION

Although metal cutting and machining have been the subject of research since the beginning of the 20th century (Taylor, 1907), they are still not well understood due to the complex, unlimited, and interrelated frictional, thermal, and tribological parameters involved in the relevant processes (Astakhov, 2006). In research on metal cutting and machining, an unsatisfactory repetitive outcome is frequently obtained with a wide domain of variation (Astakhov, 2004; Oraby & Alaskari, 2008). Therefore, real-time monitoring, diagnosis, and in-process control of the machining process may be a practical solution to most problems in metal cutting.

Numerical control (NC) of the machine tool has contributed to machining in terms of greater flexibility, better surface quality, higher dimensional accuracy, and higher productivity (Altintas, 2012). In NC technology, the required workpart's configuration is obtained through a specially written program containing special dedicated syntax information to simply guide the machine's servomotors to the target point using fixed values of cutting speed and feed rates. Such a program is prepared in advance by a qualified team with technical experience and skills related to the work material, tools type and configuration, machining features, and machinability principles. In computerized numerical control (CNC), the programmer usually chooses the feed and speed values without the flexibility to adapt to dynamic situations arising from continuous variations during cutting.

Although a few recent computer-aided-manufacturing (CAM) software have introduced tool-path optimization features to identify potential costly mistakes prior to cutting metal (Haftel, 2007), none of these products has the capability of in-process parameter adjustment to prevent unexpected premature cutting edge failure due to variations in material hardness, uneven dimensions of the workpiece, inevitable edge wear propagation, thermal stresses by cutting temperature, or fixture instability. Real-time monitoring techniques have also been introduced (OMATIVE, 2016) where the process is continuously checked before a warning alarm is activated to automatically or manually process stoppage. In tool monitoring technology, cutting loads and other influential machining outputs are assigned thresholds, above which an alarm is triggered and the process is terminated. In adaptive control systems, the feed or/and speed-controlling parameters are adjusted not to reach the thresholds. The AC system becomes even more complicated as many non-deterministic variables, such as acoustic emission and system dynamic characteristics features, become involved. As noted by Haftel, this increases system complexity with a sluggish controller, and, therefore, companies prefer to use simpler monitoring techniques than adaptive control design, which involves sophisticated instrumentation.

Adaptive control AC systems were mooted as early as 1962 (Hanson, 2014) when Bendix Corp. introduced an adaptive control optimization approach. Obstacles to the method at the time included the development of reliable sensors and other relevant instrumentation. According to Eitel (2011), early AC approaches featured standalone hardware attachments usually connected on demand to a CNC machine tool with intricate wiring that complicated the setup and slowed response. Such a controller's analog-velocity output typically went to a separate drive with a separate velocity loop that degraded system response time. Moreover, feedback loops were not always fully closed without tuning capability to compensate for errors. However, work has continued (Ulsoy et al., 1983; Chiang et al., 1995; Oraby et al., 2003; Cus et al., 2006; Haftel, 2007; Ralston &Wards, 1988; Prasad et al., 2013; Huang &Yuan, 2014; Sun et al., 2014) to develop robust, flexible AC systems and enhance their overall efficiency, especially following recent developments in the digital industry, such as superfast microprocessors and the availability of low-cost, large-capacity computer memory.

Recent adaptive control techniques (Oraby et al., 2003; Cus et al., 2006; Prasad et al., 2013; Huang &Yuan, 2014) usually involve a series of related tasks. Some process outputs (responses) are monitored in real time, followed by judgment and assessment of the outputs according to the production objectives and capabilities of the machining system. Optimization procedures are then adapted to the situation through the adjustment of one or more operative feed and speed parameters. System servomotors are then activated to perform according to the selected cutting parameters, and a feedback response is sent to the system controller for further correction and compensatory actions. While maximizing machining productivity is among the most common machining objectives, cutting forces as well as low- and high-frequency cutting vibrations are among promising measurable responses used in adaptive control systems (Oraby et al., 2003; OMATIVE, 2016; Prasad et al., 2013; Huang & Yuan, 2014).

Despite its benefits (Hanson, 2014), AC has many problems, mainly associated with the design of its controller and the high cost of the instruments required, that are obstacles to the establishment of a universally feasible commercial system.

In spite of the considerable number of studies on AC in the last decade, only three systems have been proposed for commercial application: the FANUC Adaptive Solution iAdapts (Eitel, 2011; Hanson, 2014), the TMAC system introduced by Caron Engineering (OKUMA, 2016; Albert, 2014; CARON, 2016), and Control Monitoring ACM by OMATIVE Systems (OMATIVE, 2016).

In 2010, FANUC Factory Automation America released its iAdaptS adaptive control that can be integrated on demand into the original iAdapt CNC controller (FANUC, 2011). According to FANUC, the system increases productivity through cycle time reduction by up to 40%. The system automatically optimizes the cutting feed based on spindle load. In 2012, an engineer at FANUC, Jerry Scherer, obtained a patent (US 8, 135,491 B2) for the development of its CNC adaptive control system (Goldsberry, 2012). FANUC claimed that the iAdaptS compensated for variations in material hardness, cutting edge wear, and depth or width of cut. They also indicated that their iAdaptS technique was ideal for heavy roughing operations due to its capability to withstand significant load variation due to variations in material hardness during machining. The iAdaptS AC technique usually operates at full power load to ensure maximum machining productivity. It also offers the advantage of transferring the generated cutting heat into the chips rather than the workpart, thus extending tool life (FANUC, 2011; Goldsberry 2012). Hanson (Hanson, 2014) has explained that a major advantage of iAdaptS is a dithering facility, where the feed can be adjusted to avoid dynamic instability.

Another emerging AC system is a tool-monitoring adaptive control (TMAC) recently developed by Caron Engineering (OKUMA, 2016; Albert, 2014; CARON, 2016). It claims that the TMAC provides valuable information concerning the cutting process that helps protect the CNC machine. Thus, TMAC reduces the cost associated with broken tools, lost production, and rejected parts by effectively measuring tool wear in real time (CARON, 2016). The system operates on the principle that power consumed during machining increases as the tool's cutting edges deteriorate. With the TMAC system, the cutting feed is usually regulated to maintain constant spindle motor power, thus reducing cycle time while optimizing the process to improve tool life.

Another AC system is the OMATIVE ACM that uses sophisticated algorithms to optimize the machine's programmed feed for speeding up cutting when the path is obstacle-free (air gap) and slowing down when geometry, material hardness, or tool conditions demand caution. With its features, the OMATIVE ACM is reported to reduce cycle time, increase productivity, extend tool life, and ensure consistently high-quality parts with the possibility of integration into nearly all new and old CNC machines (OMATIVE, 2016).

However, all the above AC systems usually incur high cost, and, therefore, their practical implementation remains limited to highly strategic applications where production cost is not usually of prime interest. Therefore, there is need for a cost-effective technique with a reasonable setting investment. Moreover, almost all previously developed AC approaches addressed the manipulation of only the cutting feed in end milling operations. However, cutting speed should be considered in any proposed AC strategy as a controlling parameter, since it has a dominant influence on edge wear and its rate in rough turning operations (Alajmi & Oraby, 2014; Alaskari et al., 2011).

In this study, an adaptive control simulation strategy is proposed where the core of the optimization routine is based on a previously developed mathematical empirical group of models covering a definite domain of the tool-work-machine combination. Such an approach suits situations most when the high cost of sensors and other hardware cannot be afforded. The objective is to maximize the metal removal rate (MRR) while minimizing tool wear through optimizing the speed and feed parameters under the prescribed safety limits of force and power constraints.

A series of conventional, experimental fixed-variable tests were considered to verify the effectiveness of the proposed models-based method. Outputs from both techniques were compared in terms of productivity, consumed power, edge wear level, and cutting forces. The results showed the superiority of the proposed disparate-parameter technique, which attained higher productivity due to an adequate utilization of the available power resources within a safe working environment.

Methodology and Mathematical Models

Experimental data (Oraby & Hayhurst, 1991) were used to develop mathematical models using nonlinear regression procedures. Sandvik GC435 multi-coated carbide inserts were used to dry machine 709M40 (En 19) alloy steel bars on a Colchester Mascot center lathe. A practical domain of operating parameters for rough turning was covered to include a cutting speed (V) range of 50–200 m/min, a feed (f) range of 0.06–0.6 mm/rev, and a depth-of-cut (d) range of 1.5–3 mm. The simultaneously measured variables were the nose, the flank, and notch wear scars together with three mutual force components using a specially designed three-component strain gauge dedicated dynamometer (Oraby & Hayhurst, 1990). The following significant and adequate models were developed, where (t) is the aggregate cut time in minutes:

$$Average\ Tool\ Wear\ (AW) = 7.62{\times}10^{-3} V^{0.877} f^{0.168} d^{0.248} t^{0.245}\ (mm) \quad (1)$$

with R^2=0.84, SE=0.1, F=831.

$$Consumed\ Power\ (P) = 0.14\ V^{0.82} f^{0.627} d^{0.844} t^{-0.049} AW^{0.342}\ (Kw), \quad (2)$$

with R^2=0.97, SE=0.062, F=4156.

$$Thrust\ Cutting\ Force\ (F_{xz}) = 55354\ V^{-0.484} f^{0.236} d^{0.715} t^{-0.173} AW^{1.1} (N), \quad (3)$$

with R^2=0.83, SE=0.12, F=670.

Details of the experimental procedures and the modeling criteria can be found in the work of Oraby & Hayhurst (1991).

In order to establish a reliable and more practical AC strategy, two associated issues should be borne in mind as sources of tool life variation for a given edge. The first of these is the difference in wear rate when the cutting edge is used under disparate, rather than fixed, cutting parameters where the initial wear developed in each case is different. This usually governs both the magnitude and pattern of accumulated edge wear throughout its subsequent lifespan (Oraby & Alaskari, 2008). The second source of variation is due to the fact that the standard tool life testing procedures are usually conducted based on discrete testing procedures by removing tools, normally at two- or three-minute intervals for wear measurement, after which the test is resumed. These affect the credibility of using fixed-parameter machinability data, where cutting parameters are subjected to change when the need arises. Thus, to consider the eminent variation in edge wear and its associated initial wear at the first-cut segment, the instantaneous cumulative edge wear is

$$AW_i = AW_{i-1} + \Delta W_i = AW_{i-1} + AW_{t=ti} - AW_{t=ti-1}(mm) \tag{4}$$

Substituting into Equation 1 and considering a depth of cut (*d=2.5 mm*) yield

$$AW_i = AW_{i-1} + 9.5641 \times 10^{-3} \times V^{0.577} \times f^{0.168} \times \left(t_i^{0.245} - t_{i-1}^{0.245}\right)(mm) \tag{5}$$

Substituting the instantaneous accumulated wear (AW_i) into each of Equations 2 and 3 yields

$$P_i = 0.30338 \times V^{0.82} \times f^{0.627} \times \left\{AW_{i-1} + 9.5641 \times 10^{-3} \times V^{0.577} \times f^{0.168} \times \left(t_i^{0.245} - t_{i-1}^{0.245}\right)\right\}^{0.342}(Kw) \tag{6}$$

$$F_{xz(i)} = 106580 \times V^{-0.484} \times f^{0.236} \times \left\{AW_{i-1} + 9.5641 \times 10^{-3} \times V^{0.577} \times f^{0.168} \times \left(t_i^{0.245} - t_{i-1}^{0.245}\right)\right\}^{1.1}(N) \tag{7}$$

The thrust force F_{xz} is the resultant of the feeding and radial force components; it is a sliding and frictional component and is thus most sensitive to edge wear and fracture. To avoid sudden breakage of any elements of the tooling system as well as its fixture elements, a limit of thrust force, depending on to the rigidity and stability of the machining system, should be preset.

The metal removal rate as an objective in the turning operation may be expressed as

$$Metal\ Removal\ Rate\ (MRR) = 1000\ V\ f\ d = 2500\ V\ f\ \left({mm^3}/{min}\right), \text{for } d = 2.5\ mm. \tag{8}$$

The proposed AC strategy based on mathematical models can be inserted on demand into the host computer of the CNC machine tools using the appropriate operating and controlling syntax. The proposed strategy is schematically explained in Figure 1.

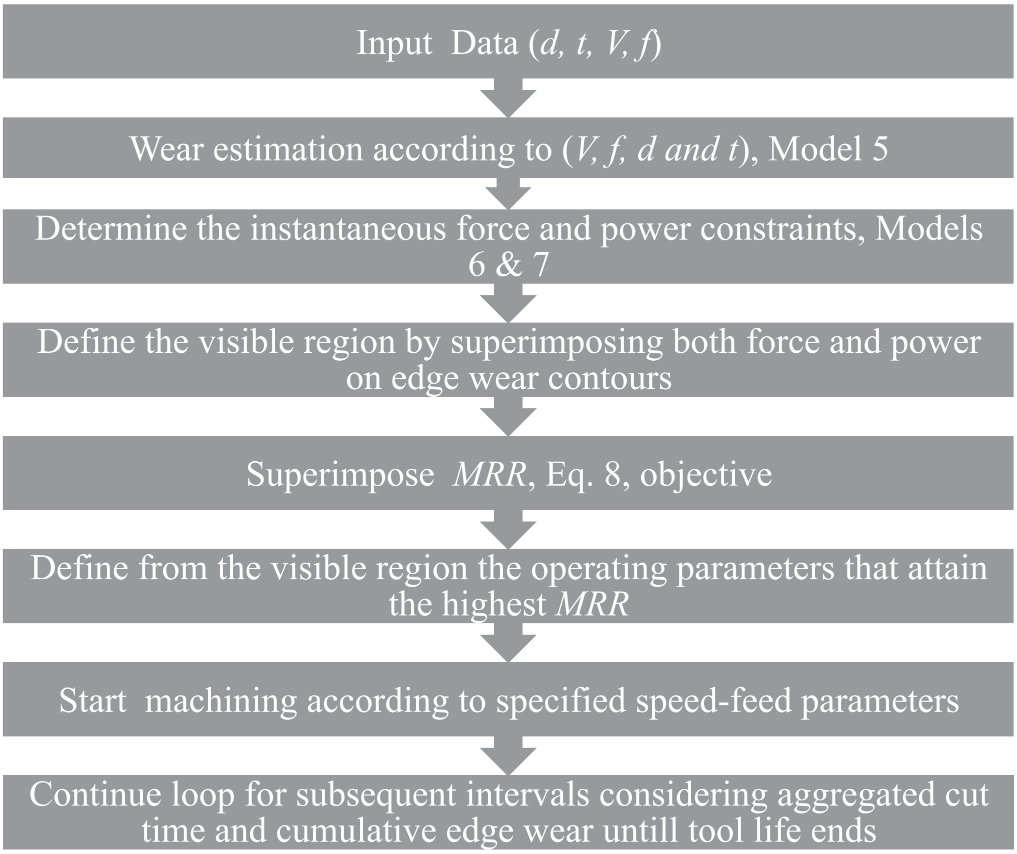

Figure 1. Flowchart indicating the proposed mathematical models-based adaptive control strategy.

RESULTS, ANALYSIS, AND EVALUATION

The algorithm iterations in this system covered all possible speed-feed combinations by considering a cutting speed range of V=50200- m/min and a feed of f=0.060.6- mm/rev. The speed and feed increments were set to 10 m/min and 0.005 mm/rev, respectively. A total of 1744 (16×109) iterations were processed for each successive sampling instance. For each speed level, a total of 109 feed values were processed to determine the corresponding edge wear, consumed power, and cutting forces together with the metal removal rate as specified by Equations 58-. Of these 109 category iterations, the maximum MRR was selected as in Table 1. The operation was repeated to cover all speed and feed domains until arriving at the stage that yielded the best results. This calculation process was recursively repeated 16 times to cover the entire speed-feed domain, as shown in Table 1. The optimum case of the 16 speed steps, which yielded the maximum MRR, was considered the stage target, and its corresponding speed-feed pair was employed through the intended interval.

Table 1. Selection of optimum operating parameters at cut time of one minute.

No.	Time (*t*) min.	Speed (*V*) m/min.	Feed (*f*) mm/rev.	Wear (*AW*) mm.	Power (*P*) kW	Force (F_{xz}) N	MRR mm^3/min
1	1	50	0.6	0.083884	2.33315679	931.248196	75000
2	1	60	0.6	0.093189	2.80865049	957.189791	90000
3	1	70	0.6	0.101858	3.28552627	979.686084	105000
4	1	80	0.6	0.110016	3.76358842	999.60018	120000
5	1	90	0.6	0.117753	4.24269023	1017.50139	135000
6	1	100	0.6	0.125133	4.72271758	1033.78604	150000
7	1	110	0.6	0.132208	5.20357911	1048.74171	165000
8	1	120	0.6	0.139015	5.68520002	1062.58402	180000
9	1	130	0.6	0.145586	6.16751794	1075.47898	195000
10	1	140	0.6	0.151946	6.65048004	1087.55733	210000
11	1	150	0.58	0.157219	6.97040767	1083.35819	217500
12	1	160	0.53	0.160731	6.99801463	1053.22409	212000
13	1	170	0.48	0.163705	6.9551237	1019.48205	204000
14	1	180	0.445	0.167056	6.99927378	996.056738	200250
15	1	190	0.410	0.169994	6.99182881	970.179811	194750
16	1	200	0.380	0.172879	6.99304131	946.940685	190000

In the following section, the proposed strategy was numerically verified for some selected intervals within the valid lifespan of the tool. Through the analysis, some technically justified assumptions were considered. The depth of cut (d) was kept fixed throughout the analysis at 2.5 mm, while the maximum allowable thrust force (Fxz) and the available spindle power (P) were limited to 1500 N and 7 kW, respectively. The criterion average edge wear (AW) level was specified as 0.3 mm as recommended by many standardization associations for single-point tools used in rough turning operations. The sampling time for each stage was one minute. However, these assumptions were used to describe the proposed strategy, which is sufficiently flexible to accept different values from the machinability database, the tools, and the materials manufacturers when technically justified.

Implementation of the proposed strategy prior to cut

The procedures started at the lowest cutting speed (V=50 m/min), and the objectives and constraints were predicted recursively for all feed ranges from f= 0.06 to 0.6 in steps of 0.005 mm/rev. Of a total of 109 process cycles, a single speed-feed combination was grasped that achieved the maximum MRR under the specified limitation of power and force (the first row in Table 1). Such procedures were recursively repeated until reaching the highest value of the speed, and the optimal speed-feed operating pair was similarly determined. Of all 16 iterations, the optimal unique operating speed-feed combination was determined by the 11th row of Table 1. As described in Figure 2, of the 16 selected optimal possibilities, the maximum MRR value of 217500 mm3/min was observed at the corresponding speed-feed combination pair of (V=150 m/min and f=0.58 mm/rev). The corresponding average edge wear (AW) was estimated according to Equation 5 as 0.157219 mm. Both power and force constraints were determined according to Equations 6 and 7 and verified to fulfill the constraints. As listed in Table 1 and Figure 2, in comparison with its value in the subsequent case, the optimum MRR value was obtained with less developed edge wear, as shown in Figure 2c, lower power consumed, as shown in Fig. 2b, and an insignificant increase in the resulting cutting forces, as shown in Figure 2a.

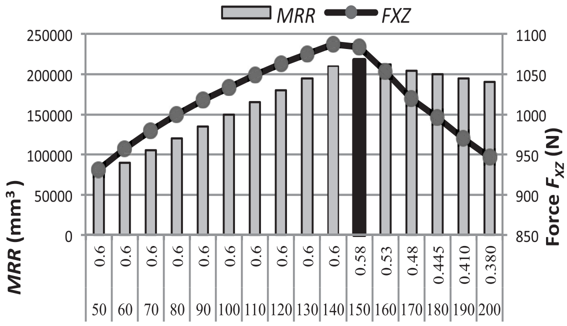

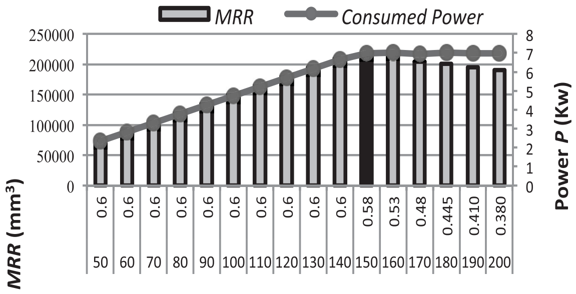

(a) Speed-feed-*MRR*-force relationship (b) Speed-feed-*MRR*-power relationship

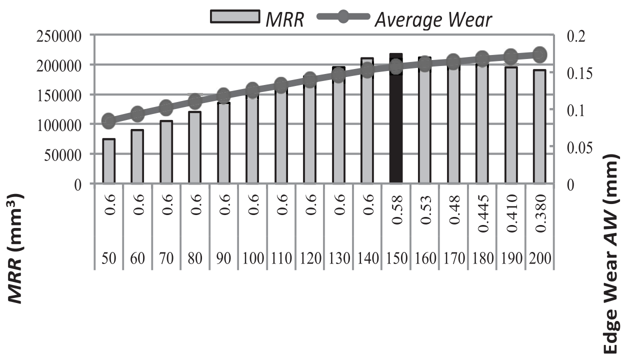

Figure 2. Output of the proposed AC strategy after one-minute machining (force, power, and wear for optimum conditions).

The proposed strategy is illustrated by Figure 3 as a contouring graph of four contours; the metal removal rate (MRR), the average wear (AW), the thrust force (Fxz), and power (P) were superimposed on one another and plotted against the valid speed-feed domain. According to the imposed force and power constraints, the visible region was bounded by ABCDEFA, as shown in Figure 3. From the infinite possibilities of speed-feed pairs within such a region, the optimal one achieved the intended objective of max MRR (point (a) in Figure 3). This located the speed-feed pair that should be used to operate the machine for the first cutting interval of one minute.

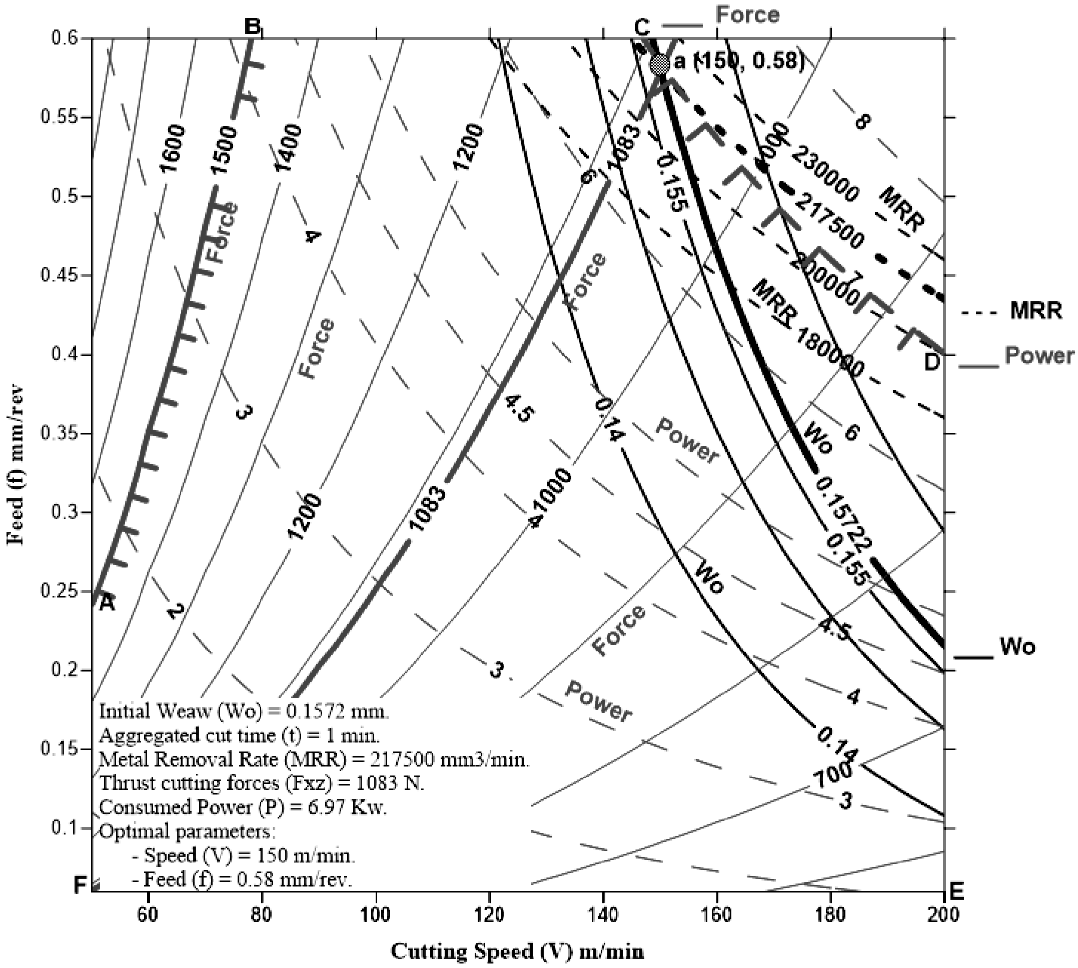

Figure 3. Contour graph of the proposed AC strategy at one-minute machining.

Implementation of the proposed strategy in subsequent cut intervals

The same procedures were repeated to find new feasible operating parameters for successive cut intervals by considering existing wear scars on the cutting edge from the past interval(s). To avoid overestimation of wear level by reconsidering the unrepeatable initial wear that was developed only in the first stage, the actual wear at any subsequent interval was estimated by considering the difference between the values at the given and the preceding intervals, in Equations 4 and 5. The results for this interval are listed in Table 2 and explained in Figure 4. Moreover, a descriptive 3D graph of the transformed data, shown in Figure 5, describes how objectives and constraints were interrelated to generate the unique operating speed-feed combination. According to the contour graphs in Figure 6, the feasibility region was determined by ABCDEFA. The cumulative edge wear at the end of these stages intersected with an MRR of 203000 mm3/min along the border of the feasibility region, as indicated by point (a) corresponding to the parameter combination pair V=140 m/min and f=0.58 mm/rev.

Once again, the benefit of the proposed strategy in optimizing productivity was evident, since the obtained MRR was greater than its value in either preceding or subsequent cases, as shown in Table 2 and Figure 4, with an unnoticeable change in the value of the edge wear and in the consumed power. Moreover, the resulting force values at the selected point were found less than those for the preceding loop, which yielded a lower MRR. Within this interval and due to added edge wear scars, speed was reduced with an expected increase in force level.

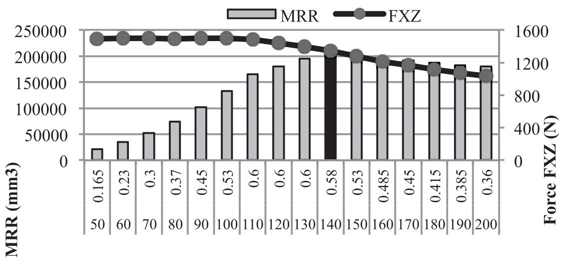

(a) Speed-feed-*MRR*-force relationship

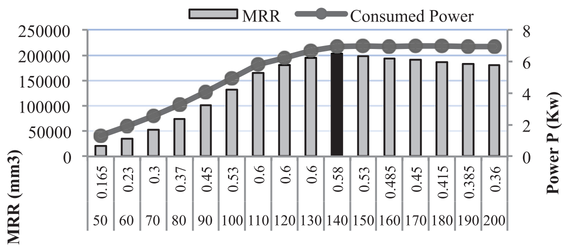

(b) Speed-feed-*MRR*-power relationship

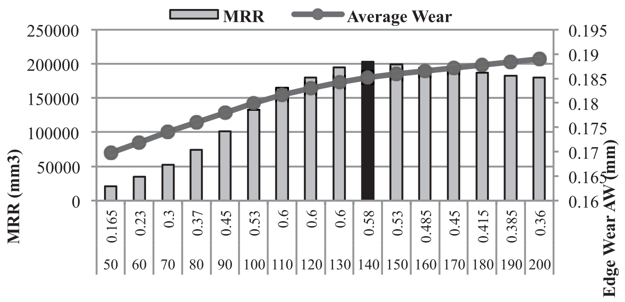

(c) Speed-feed-*MRR*-wear relationship

Figure 4. Output of the proposed AC strategy after two-minute machining (force, power, and wear for optimum conditions).

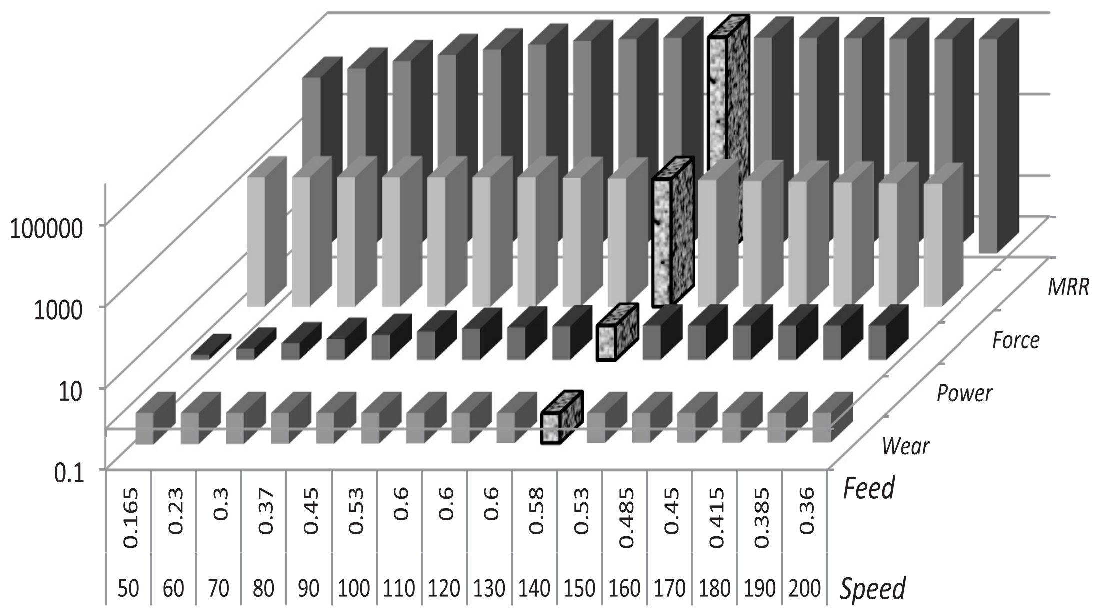

Figure 5. A three-dimension representation of the objectives and constraints of the proposed AC system to select operating parameters for the second minute.

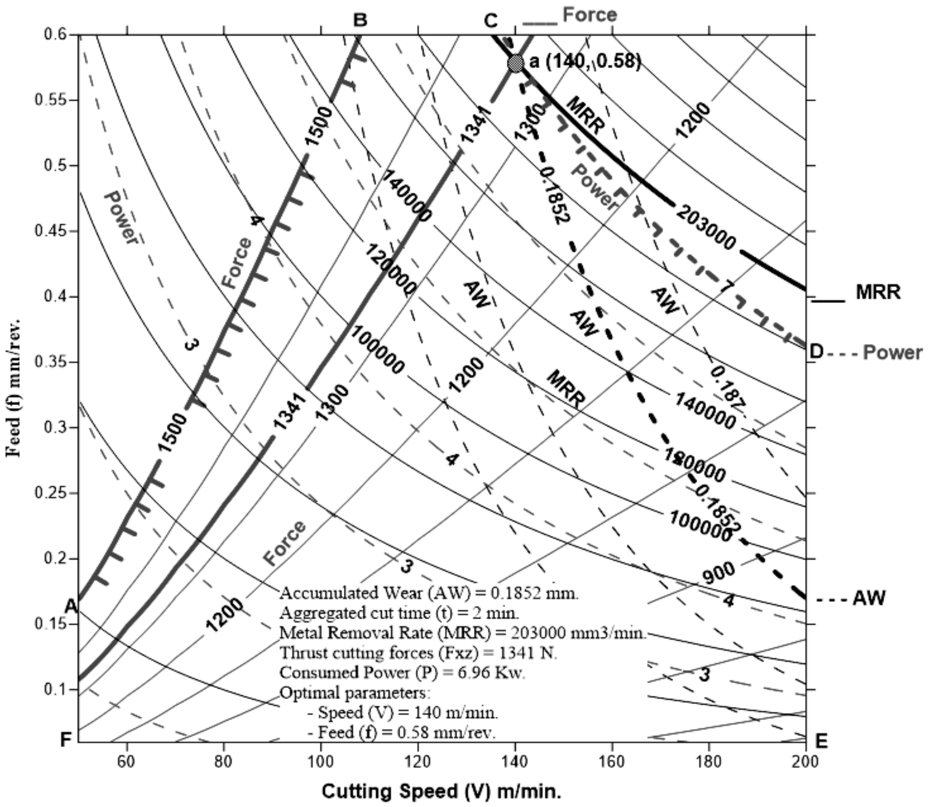

Figure 6. Contour graph of the proposed AC strategy at two-minute machining.

Table 2. Selection of best operating parameters at cut time of two minutes.

No.	Time (t) min.	Speed (V) m/min.	Feed (f) mm/rev.	Past Accum. Wear mm.	Initial Wear Wo_i mm.	Initial Wear Wo_i-1 mm.	Wear increase mm.	Total Wear (AW) mm.	Power (P) kW	Force (F_{xz}) N	MRR mm^3/min.
1	2	50	0.165	0.157219	0.08003	0.06753	0.01255	0.16972	1.32	1491	20625
2	2	60	0.23	0.157219	0.09401	0.07932	0.01468	0.17190	1.90	1497	34500
3	2	70	0.3	0.157219	0.10744	0.09066	0.01678	0.17400	2.56	1499	52500
4	2	80	0.37	0.157219	0.12021	0.10143	0.01877	0.17599	3.26	1495	74000
5	2	90	0.45	0.157219	0.13296	0.11220	0.02077	0.17799	4.08	1498	101250
6	2	100	0.53	0.157219	0.14524	0.12255	0.02268	0.17990	4.95	1497	132500
7	2	110	0.6	0.157219	0.15668	0.13221	0.02447	0.18169	5.80	1488	165000
8	2	120	0.6	0.157219	0.16474	0.13901	0.02573	0.18295	6.24	1437	180000
9	2	130	0.6	0.157219	0.17253	0.14559	0.02695	0.18417	6.68	1393	195000
10	2	140	0.58	0.157219	0.17905	0.15108	0.02796	0.18519	6.97	1341	203000
11	2	150	0.53	0.157219	0.18352	0.15486	0.02866	0.18589	6.98	1275	198750
12	2	160	0.485	0.157219	0.18766	0.15835	0.02931	0.18653	6.97	1215	194000
13	2	170	0.45	0.157219	0.19191	0.16194	0.02997	0.18719	6.99	1164	191250
14	2	180	0.415	0.157219	0.19567	0.16511	0.03056	0.18778	6.97	1114	186750
15	2	190	0.385	0.157219	0.19934	0.16821	0.03113	0.18835	6.96	1070	182875
16	2	200	0.36	0.157219	0.20302	0.17131	0.03171	0.18893	6.97	1031	180000

Implementation of the proposed strategy prior to the end of tool life

Procedures continued progressively at the prescribed time increment until arriving at a criterion wear level of 0.3 mm. The following is an explanation of the strategy procedures by considering a late stage of machining, after which the cutting edge came to the end of its specified useful life.

Due to the highly developed edge wear, the process adapted its requirements of maximum MRR within the allowable force constraint limit, as in Figures 7 and 8. As the visible region narrowed, ABCA in Figure 7, the best operating parameters were determined as point (B) corresponding to the (200, 0.205) speed-feed pair. As shown in Figure 8a, unacceptable force levels were obtained at up to a cutting speed of 100 m/min. However, the force limit was maintained at higher levels of cutting speed with a noticeable increase in the consumed power and the developed edge wear.

This stage represented the boot to enter into the critical stage, where it was expected that the edge wear would surpass its criterion limit. This was explained by evaluating the results of the processing of the subsequent interval, as shown in Figures 9 and 10.

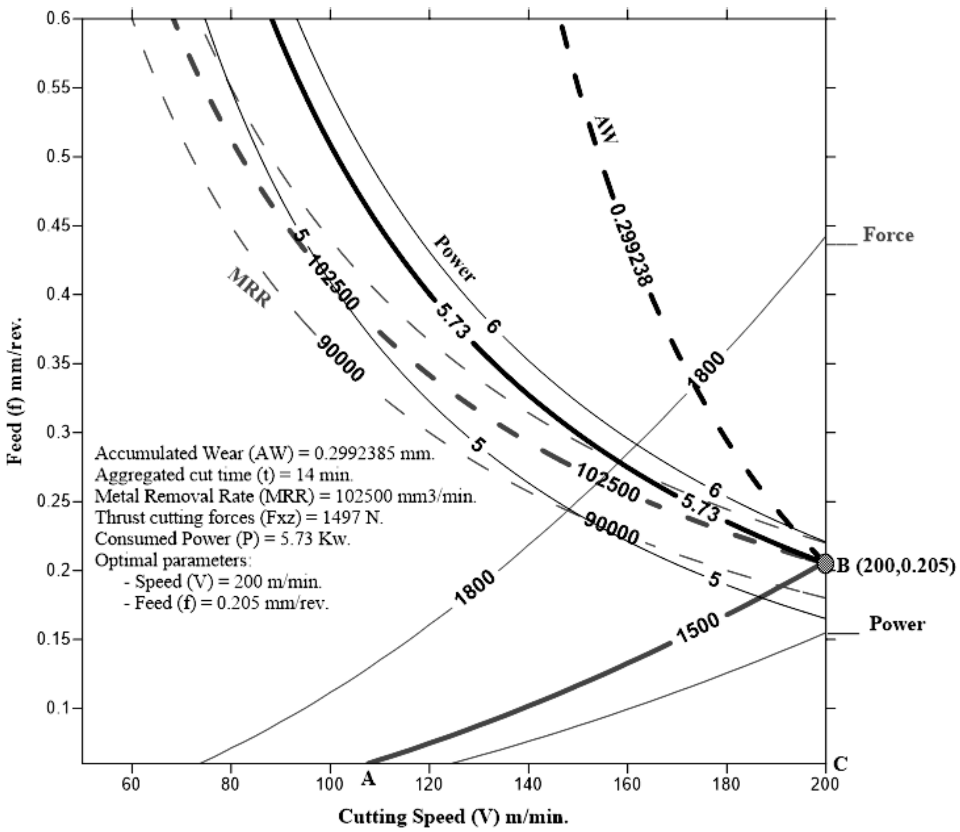

Figure 7. Contour graph of the proposed AC strategy at 14-minute machining.

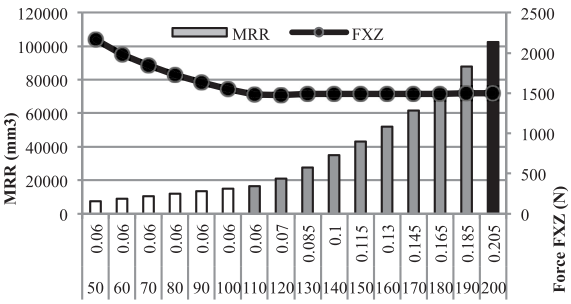

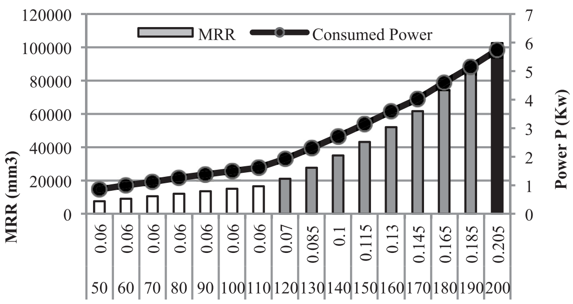

(a) Speed-feed-*MRR*-force relationship (b) Speed-feed-*MRR*-power relationship

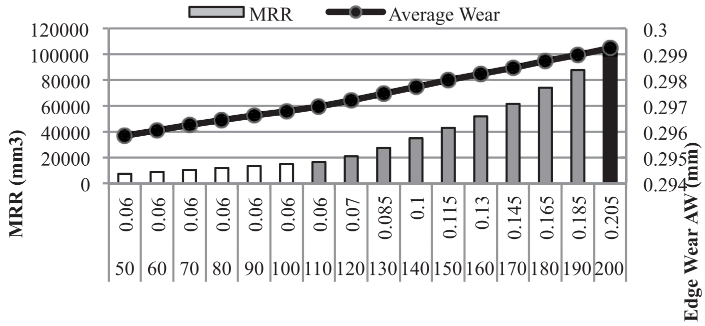

(c) Speed-feed-*MRR*-wear relationship

Figure 8. Output of the proposed AC strategy after 14-minute machining.

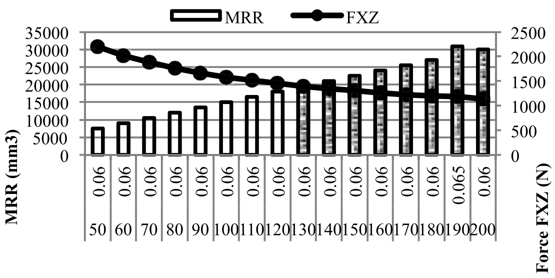

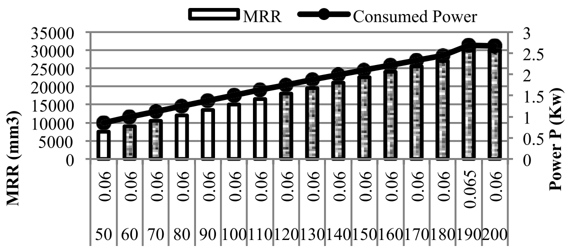

(a) Speed-feed-*MRR*-force relationship(b) Speed-feed-*MRR*-power relationship

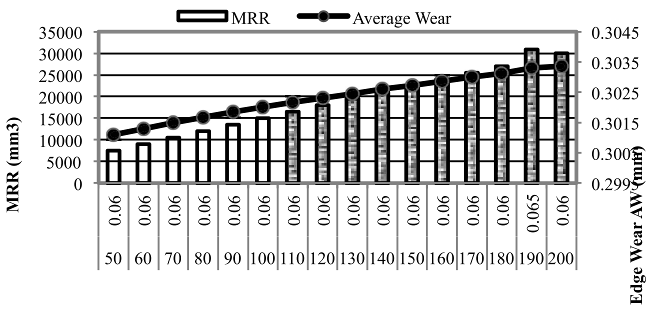

(c) Speed-feed-*MRR*-wear relationship

Figure 9. Output of the proposed AC strategy at the end of tool life.

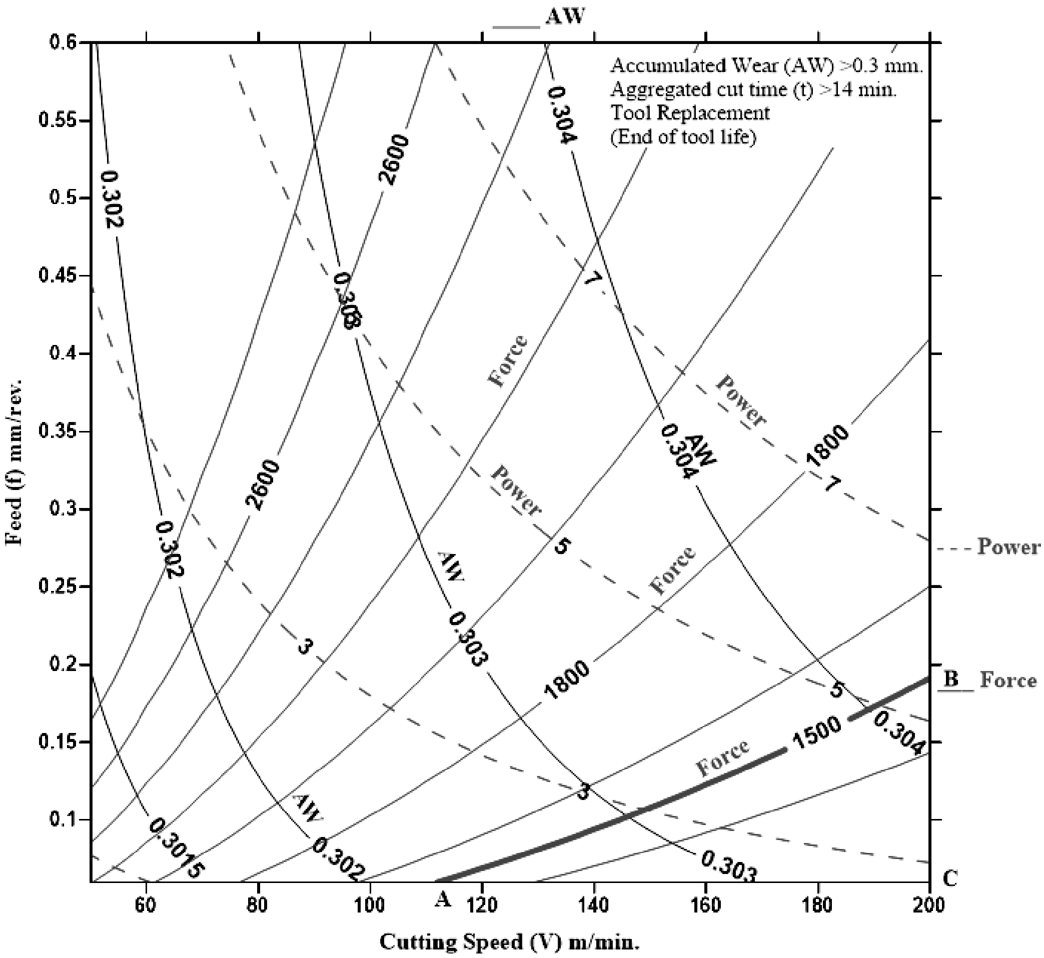

Figure 10. Contour graph of the proposed AC strategy at the end of tool life.

As shown in Figure 9c, all possible operating parameters were above the specified edge wear constraint value of 0.3 mm. implying the end of the tool life. Such prior information showed the importance and benefits of the proposed system in avoiding entering unsafe operating conditions that incur a greater likelihood of edge fracture and deformation. As shown in Figure 9, the criterion wear limit was reached, although the forces and power constraints were still well below their upper limits. As shown by the contour graph in Figure 10, the visible region vanished as the wear contour entered the operating speed-feed plane with a higher value than the criterion limit.

General Discussion and Assessment

General assessment and evaluation of the proposed strategy

Figures 11 and 12 show the entire set of the operating parameters throughout the different stages until tool life terminated. We observed that the MRR quantity obtained gradually diminished as the cutting edge practiced an escalating amount of wear scars, or as it became less steady, as shown in Figure 11c. The wider wear land generated more severe friction on the tool-workpiece interface, leading to higher force values, as in Figure 11a. This is called for compensatory technical action in terms of lower feed values, as in Figure 12. As a primary governing parameter of the cut area, the decreasing feed trend tended to have a greater effect on the MRR than the cutting speed. Feed began at a value of 0.58 mm/rev down to only 0.205 mm/rev at the last interval, when the edge wear almost reached its criterion value. On the contrary, the cutting speed tended to continuously increase, and this, on the one hand, increased the metal removal rate and, on the other, helped maintain the resulting force within the safe limit. In general, the visible economical operating region in the proposed strategy is bound by a speed range (140200- m/min) and a feed range (0.205-0.58 mm/rev). As indicated in Figure 11b, the proposed strategy indicated a promising capability to optimize the use of the available spindle power at its upper level, except in the late stages when the edge wear reached a crucial level, at which the tool was exhausted and, consequently, conservative performance and special attention were required.

Finally, the proposed approach introduced a flexible strategy to explain how to use the mathematical (empirical) interrelationships to establish a practical adaptive control system for higher productivity, fewer stopping interruptions, and better safety by the optimal utilization of the available resources. Mathematical or empirical models can be easily developed and updated using many sources, such as machinability databases, technical data from tools and materials' manufacturers, and even machinability testing procedures. The proposed strategy together with its algorithm software is beneficial whenever the high cost of sensors, transducers or, other control hardware cannot be afforded. Sensors and other hardware can be further integrated into the proposed strategy, which provides an opportunity to enhance the overall performance of the adaptive control system. Force and/or power measurement in real time can be used to subsidize empirical predictability.

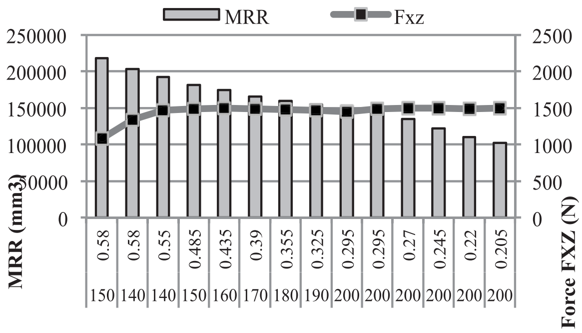

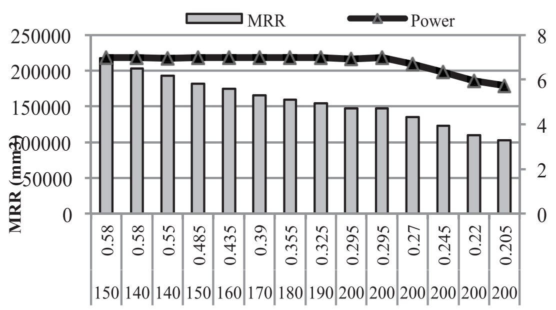

(a) *MRR* through force constraint (b) *MRR* through power constraint

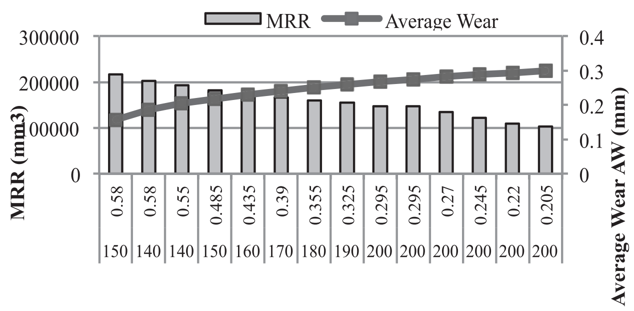

(c) Progressive edge wear and *MRR* though tool lifespan

Figure 11. MRR distributions through tool life under force and power constraints.

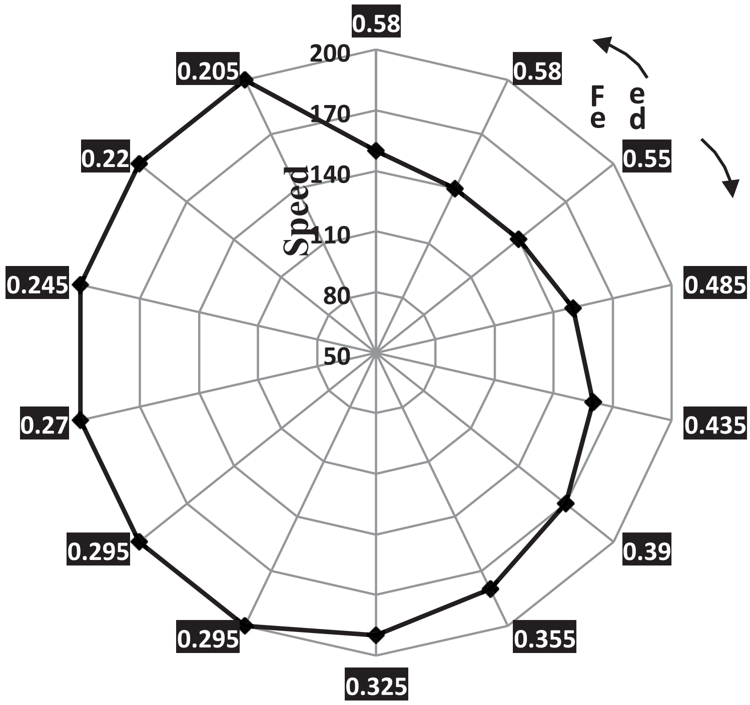

Figure 12. Disparate speed-feed operating parameters along successive cut intervals throughout tool lifespan according to the proposed AC strategy.

Experimental verification of the proposed strategy

In order to highlight the benefits of using the disparate-parameter AC procedures over the conventional fixed-parameter machining, a set of wear-time machinability experiments were performed. This included conducting nine tests to cover the domain of feasible parameters, within which the proposed AC strategy was activated.

The selection of proper mating speed-feed parameters is not always easy and requires extensive technical experience and deep knowledge of the relevant machinability database. While the edge wear rate together with the consumed power was greatly influenced by the cutting speed employed, the MRR and process productivity were mainly determined by the level of feed.

The parameters domain of the verification experiments included ranges of 100206- m/min, 0.06-0.6 mm/rev., and 1.53- mm for cutting speed, feed, and depth of cut, respectively. Experimental wear-time results of the nine experiments are shown in Figures 13a, 14a, and 15a. The outputs of the proposed AC disparate-parameter procedures also superimposed each set of data in each case for the sake of technical comparison.

Figure 13a shows the experimental wear-time results for four fixed-parameter experiments at a cutting speed of 100 m/min using 0.060.6- mm/rev. and 1.53.0- mm as feed and depth of cut, respectively. The intersection of the criterion of wear level with each curve determined the real tool life. Functional and performance comparisons between the outputs from the fixed-parameter machining of the given group and those from the disparate-parameter AC machining are shown in Figure 13b. This included the tool lifespan, productivity or MRR per minute of cutting, the resulting thrust force, and the consumed power. To include all such dissimilar parameter ranges in the same graph, a logarithmic scale for the vertical axis was considered with data value being indicated for each series. It is clear that the average productivity of the AC disparate-parameter machining yielded 10.6, 4.79, 3.19, and 1.06 times greater productivity per minute than T1, T2, T3, and T4, respectively. Although the performance of the AC strategy appeared close to that of T4, which attained 11 minutes' tool life, the overall productivity of AC at its tool life end was still approximately 1.45 times superior in terms of metal removal. However, the comparison of test productivity depending on edge life period was not completely accurate. With today's low-cost, hard, and tough cutting inserts, total production costs rate considering the expense of other machining elements, such as labor and consumed energy, becomes a prime concern. A shorter life with a high feed-depth combination may lead to better productivity using one or more edges. Furthermore, the cost of the tool replacement cycle is tremendously reduced, as it is now simple to automatically switch between two or more mating inserts in the machine turret. In rough cutting, the edge wear is no longer a crucial factor by itself, but the problem lies in the accompanying technical consequences. An increased emerging edge wear usually escalates the cutting forces and the consumed power. As indicated in Figure 13b, the greater consumed power at controlled force level for the AC machining emphasized its main feature of the optimal utilization of the available system power resources to achieve its main goal of maximizing productivity without violating safety considerations. It is, in general, unwise to take a conservative technical decision while a highly rigid and stable system may afford better productivity.

Another verification group was considered using a higher level of cutting speed of 145 m/min, as demonstrated in three more verification experiments, T5 to T8, in Figure 14. As shown in Figure 14b, it was observed that experiment T8 yielded almost half the life of the AC disparate-parameter machining with only approximately 73% of its productivity per minute of cutting. This implies that, at the end of tool life of the two trials, AC machining was 2.94 times higher in terms of accumulated productivity than conventional fixed-parameter testing. Moreover, although the experiment T5 yielded an edge life of 15 minutes of cutting, it achieved approximately 58% of the productivity attained by the AC strategy, as shown in Figure 14b. It was also evident that, in all fixed non-adaptive experiments—T5, T6, T7, and T8—the available machine power was not optimally exploited to enhance productivity.

Further analysis and verification were performed by considering a higher level of cutting speed of 206 m/min, in test T9, as shown in Figure 15. During the experiment, the cutting edge catastrophically failed (plastic deformation) after only 6.25 min of cutting, as shown in Figure 15a. The AC disparate-parameters were 61% higher in productivity per minute of cutting than the fixed-parameter machining, T9. This implied that the total productivity of AC strategy was approximately 4.83 times that of conventional machining. Furthermore, the conventional fixed-parameter test T9 generated an aggressive force level of 2690 N at the failure instant, which jeopardized the tooling clamping system and its fixture elements as well as the operator's safety.

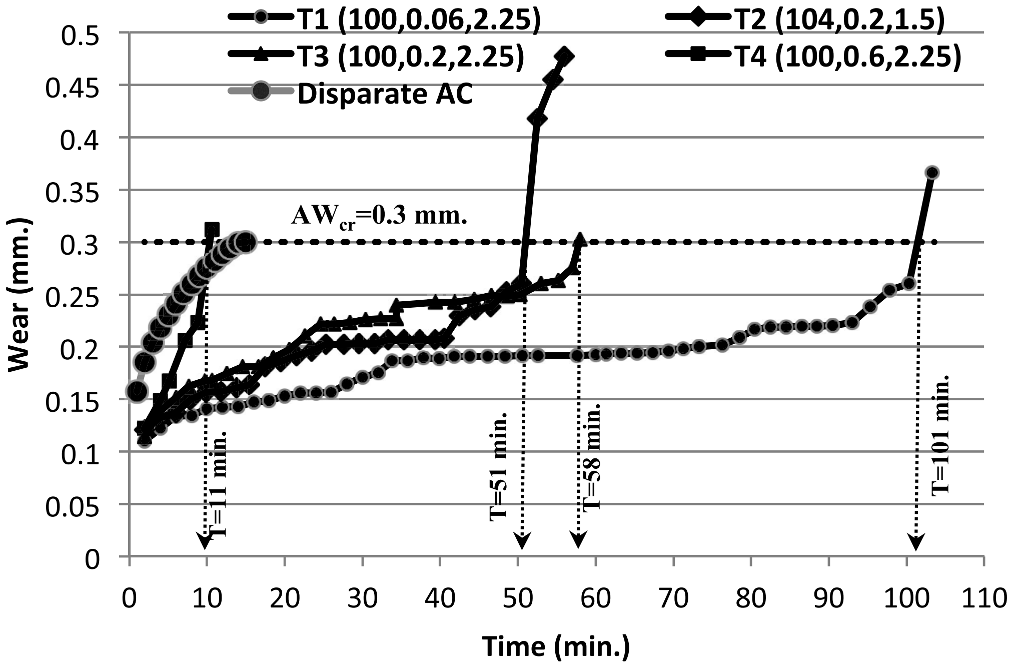

a) Wear-time experimental testing.

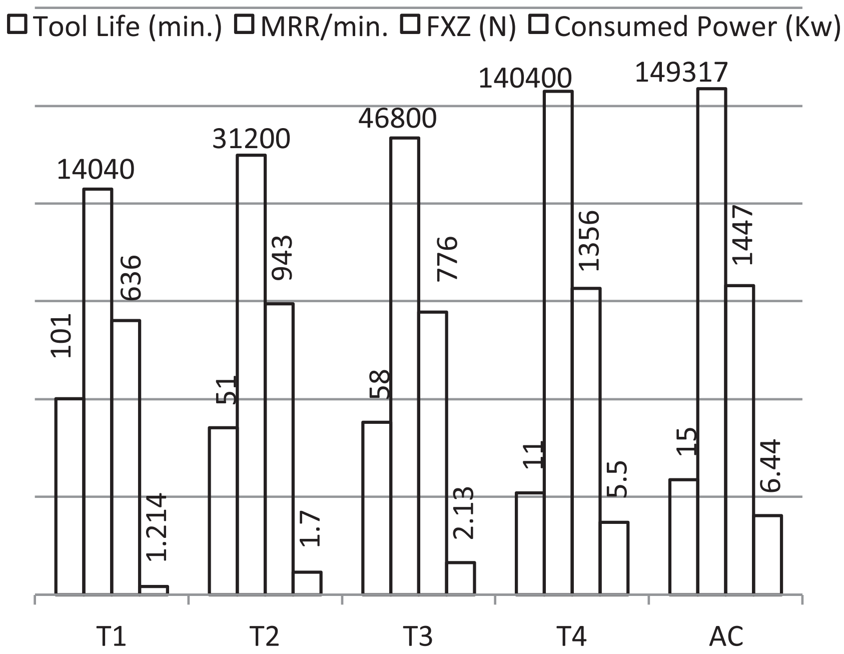

b) Machining outputs of fixed and AC disparate-parameter.

Figure 13. Experimental verification of productivity at cutting speed of 100 m/min.

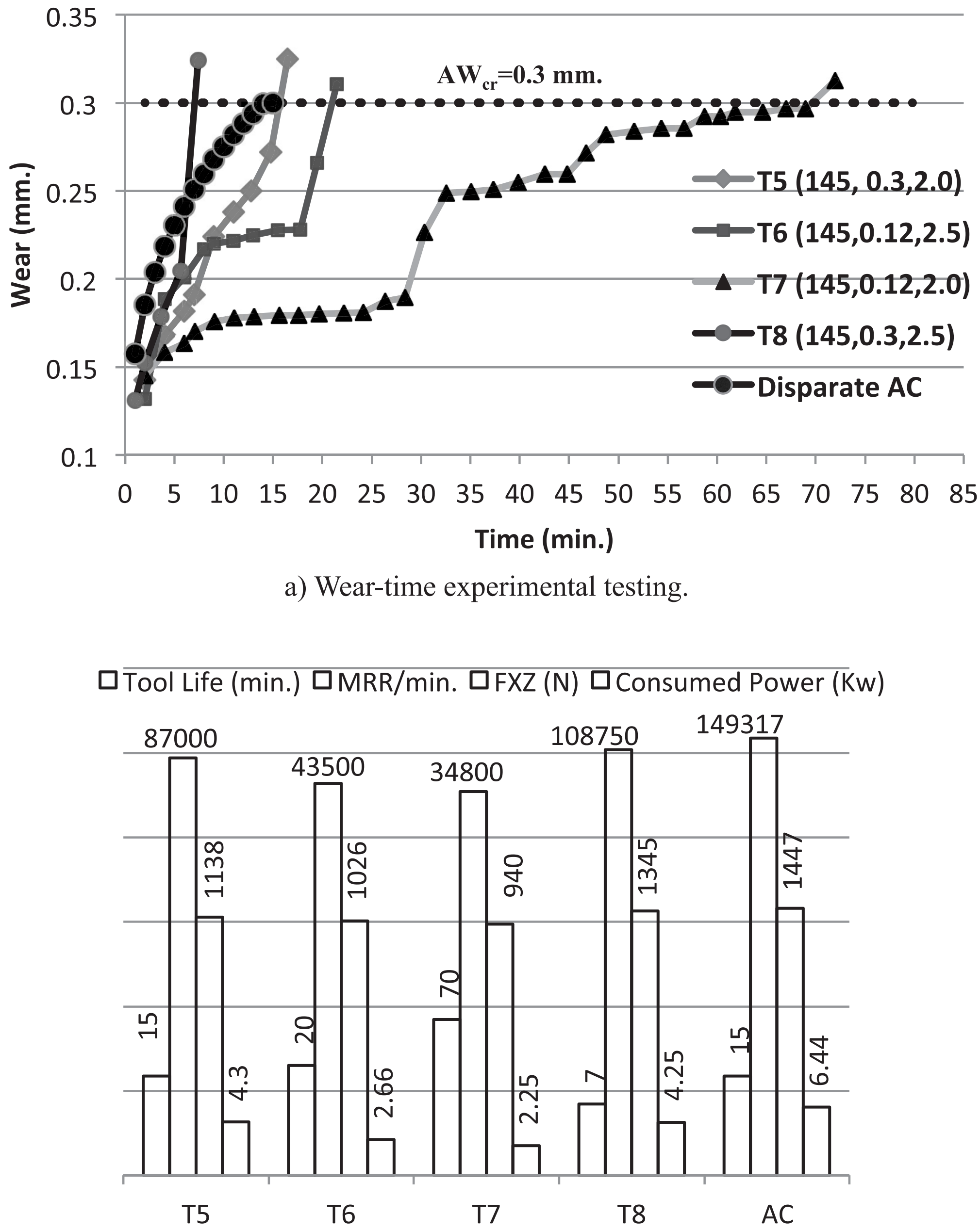

a) Wear-time experimental testing.

b) Machining outputs of fixed and AC disparate-parameter.

Figure 14. Experimental verification of productivity at cutting speed of 145 m/min.

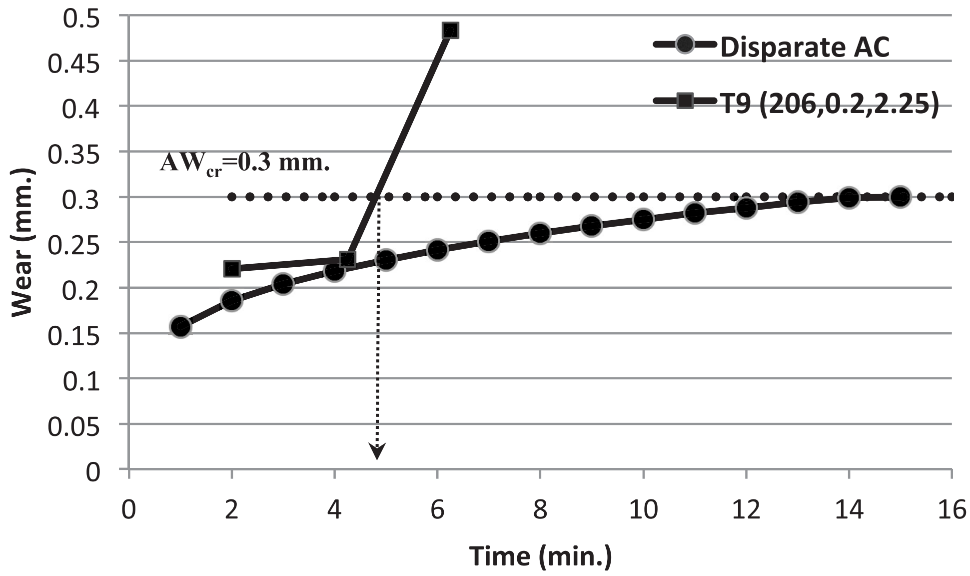

a) Wear-time experimental testing.

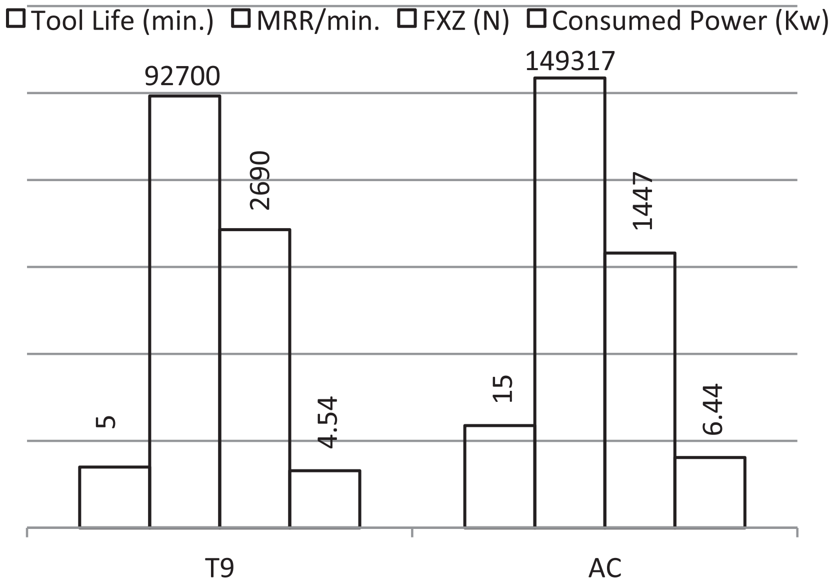

b) Machining outputs of fixed and AC disparate-parameter.

Figure 15. Experimental verification of productivity at cutting speed of 206 m/min.

Conclusions

With the development of progressive edge wear, all process responses and outputs in machining are no longer invariable, and the fixed cutting parameters prescribed in the NC parts program are hence no longer valid. The problem worsens as direct measurement of edge wear is not yet possible. Assuming improper operating parameters usually reduces productivity and jeopardizes both the system and the operator's safety. Therefore, real-time techniques are needed to monitor and control the manufacturing process.

An adaptive control mathematical models-based strategy was proposed in this study to monitor and control the rough turning machining operation. At specified cut intervals, edge wear is assessed using the appropriate relevant empirical model. The goal was to achieve the maximum metal removal rate by selecting the instantaneous best speed and feed operating parameters without violating system safety and power capability.

Many statistical, analytical and graphical programs were used throughout the analysis to examine the viability of the proposed strategy. The use of the proposed strategy allowed for a safer environment than in case of random operating parameters, with fewer stoppings and shorter downtime. The performance of the proposed models-based method was verified by comparing its productivity with that of several fixed-parameter wear-time experiments, and the results indicated its superiority. As the entire available machining power was feasible, the AC process yielded up to 10.6 times greater metal removal rate with a huge reduction of the tool replacement cycle cost. Also, a safe machining environment for both operators and machine elements is guaranteed.

The proposed AC approach is sufficiently flexible to suit any further input with different objective, constraints, or even criteria, and limits whenever justified technical information is available. It can be properly inserted into conventional NC parts programs using appropriate syntax and programming features to create novel AC-NC mathematical models-based multi-response multi-constraint techniques.

Acknowledgment

The authors thank the Public Authority for Applied Education and Training (PAAET), Kuwait, for funding this research under the support agreement (TS-14-14).

References

Alajmi, M.S. & Oraby, S.E. 2014. On the influence of the speed-feed interaction on the wear rate and life of multiple coated carbide inserts considering rough turning process. Applied Mechanics and Materials. Trans Tech Publications **575**: 431–6.

Alaskari, A. M. Oraby, S. E. & Al-Khalid, H. K. 2011. Mathematical Modeling Experimental Approach of the Friction on the Tool-Chip Interface of Multicoated Carbide Turning Inserts. International Journal of Advances in Machining and Forming Operations **3**(2): 167-83.

Albert, M. 2014. Tool monitoring for multitasking machines. Modern Machine Shop. www.mmsonline.com/articles/tool-monitoring-for-multitasking-machines, [Sep. 1, 2016].

Altintas Y. 2012. Manufacturing Automation: metal cutting mechanics, machine tool vibrations, and CNC design. Second edition. Cambridge University Press. Cambridge UK.

Astakhov, V.P. 2004. The assessment of cutting tool wear. International Journal of Machine Tools and Manufacture **44(**6): 637–47.

Astakhov, V.P. 2006. Tribology of Metal Cutting. Elsevier. San Diego CA USA.

CARON™, 2016. Tool monitoring adaptive control. Caron Engineering, www.caroneng.com/products/tmac-mp, [Sep. 1, 2016].

Chiang, S.T., Liu, D.I., Lee, A.C. & Chieng, W.H. 1995. Adaptive control optimization in end milling using neural networks. International Journal of Machine Tools and Manufacture **35**(4): 637–60.

Cus, F., Zuperl, U., Kiker, E. & Mllfelener, M. 2006. Adaptive controller design for feed rate maximization of machining process. Journal of Achievements in Materials and Manufacturing Engineering **17**(140–237 :(2-.

Eitel, L. 2011. Adaptive control in machining-motion system design. Machine Design. machinedesign.com/sensors/adaptive-control-machining, [Sep. 1, 2016].

FANUC™, 2011. FANUC integrates iAdaptS controller into CNC. Automation. www.automation.com/product-showcase/fanuc-integrates-iadapts-controller-into-cnc, [Sep. 1, 2016].

Goldsberry, C. 2012. Fanuc FA America awarded new patent. Plastics Today. www.plasticstoday.com/fanuc-fa-america-awarded-new-patent/47176791217511, [Sep. 1, 2016].

Haftel, L. 2007. Adaptive controls save tools and time—Technology advances supercharge an old process. American Machinist. www.americanmachinist.com/machining-cutting/adaptive-controls-save-tools-and-time, [Sep. 1, 2016].

Hanson, K. 2014. Adapt and conquer. Cutting Tool Engineering. www.ctemag.com/news-videos/articles/adapt-and-conquer, [Sep. 1, 2016].

Huang, Y. & Yuan, J .2014. High-speed constant force milling based on fuzzy controller and BP neural network. International Journal of Control & Automation **7**(5): 143–52.

OKUMA™, 2016. Software automates tracking of tool wear and reduces operator costs. Okuma the Americas. www.okuma.com/software-automates-tracking-of-tool-wear-and-reduces-operator-costs [Sep. 1, 2016].

OMATIVE™, 2016. Adaptive control and monitoring. OMATIVE Systems, Internet: www.omative.com/ACM.html [Sep. 1, 2016].

Oraby, S.E. & Hayhurst, D.R. 1991. Development of models for tool wear force relationships in metal cutting. International Journal of Mechanical Sciences **33**(2): 125–38.

Oraby, S.E. & Hayhurst, D.R. .1990. High-capacity compact three-component cutting force dynamometer. International Journal of Machine Tools and Manufacture, **30**(4): 549–59.

Oraby, S.E. & Alaskari A.M. 2008. On the variability of tool wear and life at disparate operating parameters. Kuwait Journal of Science &Engineering, **35**(1B): 123–50.

Oraby, S.E., Almeshaiei, E.A. & Alaskari, A. 2003. An adaptive control simulation approach based on a mathematical model optimization algorithm for rough turning. Kuwait Journal of Science & Engineering **30**(2): 213–34.

Prasad, B.S., Prasad D.S., Sandeep A. & Veeraiah, G. 2013. Condition monitoring of CNC machining using adaptive control. International Journal of Automation and Computing **10**(3): 202–9.

Ralston, P.A.S. & Wards T.L. 1988. Mathematical models used for adaptive control of machine tools. Mathematical and Computer Modelling **11**: 1151–55.

Sun, Y., Zhao, Y., Bao, Y. & Guo, D. 2014. A novel adaptive-feed rate interpolation method for NURBS tool path with drive constraints. International Journal of Machine Tools and Manufacture **77**: 74–81.

Taylor, F.W. 1907. On the art of metal cutting. Transactions American Society of Mechanical Engineers **28**: 31–50.

Ulsoy, A.G., Koren, Y. & Rasmussen, F. 1983. Principal developments in the adaptive control of machine tools. Journal of Dynamic Systems, Measurement and Control **105**(2): 107–12.

Submitted: 18/03/2017
Revised : 13/06/2017
Accepted : 16/06/2017

Journal of Engineering Research **Vol. 6 No. (2) June 2018 pp.** *231*

محاكاة تحكم تكيفية
لتحسين إزالة المعادن لخراطة التخشين

أ يمن العسكري و سامي عرابي

قسم هندسة تكنولوجيا التصنيع ، كلية الدراسات التكنولوجية، الهيئة العامة للتعليم التطبيقي والتدريب، ص. ب. 42325 الشويخ 70654، الكويت

الخـلاصـة

في عملية التحكم العددي التقليدي، لا يمكن تغيير معلمات التشغيل المُعدة مسبقاً في البرنامج أثناء دورة التشغيل. وعلى النقيض من ذلك، تستخدم تقنية التحكم التكيفي نظام الاستشعار اللحظي لضبط التغذية التشغيلية و / أو معلمات السرعة بشكل فوري ومستمر إلى مستوياتها المثلى لضمان عملية تشغيل أكثر إنتاجية. في هذه الدراسة، تم اقتراح استراتيجية محاكاة لعملية تحكم تكيفي ترتكز على النمط لتحسين عملية إزالة المعادن أثناء خراطة التخشين عن طريق استخدام موارد الطاقة المتوفرة داخل بيئة التشغيل الآمنة بكفاءة. يستند هذا النهج على تكرارات مستمرة للتنبؤ بالمستوى اللحظي لإنهاك الحواف، جنباً إلى جنب مع قوى القطع والطاقة المستهلكة المماثلة، من خلال النظر في النماذج ذات الصلة. تم اختيار أفضل زوج تغذية للسرعة والذي يوفر أقصى معدل إزالة للمعادن دون انتهاك القوى المفروضة والقيود على الطاقة. يتم تكرار الإجراءات لفترات قطع لاحقة عن طريق النظر إلى تآكل الحافة التراكمي من فترات سابقة حتى يصل مستوى تآكل الحافة المتراكم إلى قيمة المعيار المحددة. تم التحقق من أداء الأسلوب القائم على النموذج المقترح من خلال المقارنات مع العديد من طرق المعلمات الثابتة وزمن التآكل التقليدية. أثبتت النتائج تفوق الإجراءات المقترحة لمعايرة التيار المتردد من حيث زيادة الإنتاجية بشكل ملحوظ حيث تم استغلال كامل طاقة الماكينة المتوفرة مع بيئة تشغيل آمنة مع انخفاض تكلفة دورة الاستبدال.